IEEE Access
Multidisciplinary | Rapid Review | Open Access Journal

Received July 18, 2020, accepted September 3, 2020, date of publication September 7, 2020, date of current version September 21, 2020.

Digital Object Identifier 10.1109/ACCESS.2020.3022395

Flocking for Multiple Subgroups of Multi-Agents With Different Social Distancing

HUI WEI AND XUE-BO CHEN
School of Electronic and Information Engineering, University of Science and Technology Liaoning, Anshan 114051, China
Corresponding author: Xue-Bo Chen (xuebochen@126.com)

This work was supported in part by the Funds of the National Natural Science Foundation of China under Grant 71571091 and Grant 71771112, and in part by the University of Science and Technology Liaoning Talent Project under Grant 601011507-03.

ABSTRACT In this paper, considering the difference in social distancing among individuals, according to the extent of social distancing, a group composed of N mobile agents is divided into multiple different subgroups. Especially, from the perspective of differential game theory, the flocking problem of different subgroups can be regarded as collision avoidance between neighboring agents, or obstacle avoidance between agents and virtual static/dynamic obstacles. To explore the internal mechanism of this interesting problem, a novel flocking algorithm with multiple virtual leaders is designed. The proposed algorithm is a modified version of the traditional flocking and semi-flocking algorithms. Based on the Lyapunov stability theorem and LaSalle's invariance principle, the stability analysis of the proposed algorithm is then proven. Furthermore, considering the complex environment that swarm robots or unmanned aerial vehicles (UAVs) may face when performing military missions such as surveillance, reconnaissance, and rescue, etc., we also investigate the flocking problem of multi-agents in both virtual static and dynamic obstacles environment. Finally, three kinds of simulation results are provided to demonstrate the effectiveness of the proposed results.

INDEX TERMS Flocking, multi-agent systems, collision avoidance, obstacle avoidance, social distancing.

I. INTRODUCTION

Flocking (or collective behavior), a common phenomenon in nature, is characterized by self-organization, local interaction, and decentralization [1]–[3]. Examples of this phenom include such as fish schools, bird flocks, ant colonies, and bacteria swarms, etc. Due to its broad applications in fields such as multi-target tracking of mobile sensor networks [4]–[6], cooperative control of swarm robots [7]–[9], and coordinated motion of unmanned aerial vehicles [10]–[12], etc., the flocking of multi-agents has attracted a great deal of attention among researchers from different disciplines [13]–[24].

In 1986, Reynolds proposed three heuristic rules of the flocking: *flock centering*, *collision avoidance*, and *velocity matching*, and especially, he pioneered a computer model for simulating flocks of birds [13]. Since then, inspired by Reynolds' rules, theoretical investigations on the flocking of multi-agents have achieved fruitful outcomes. For example, in 1995, Vicsek *et al*. [14] provided a self-driven particle model, also known as the Vicsek model, to investigate the flocking, transfer, and phase change of non-equilibrium systems. From the matrix theory (especially, the non-negative matrix theory), in 2003, Jadbabaie *et al*. [15] first proposed the mathematical proof of the Vicsek model, which greatly promoted the research on consistency and coordinated control for multi-agent systems. Soon after, Tanner [16] designed a decentralized control protocol to enable a group of vehicles to move as a flock, this protocol consists of a gradient-based term and velocity consensus term. Whereas Olfati-Saber suggested that navigational feedback should be added to determine the fragmentation of the initial states, thereby, Olfati-Saber provided a theoretical framework for the design and analysis of flocking for multi-agent systems [17]. However, since the flocking algorithm proposed in [17] requires substantial communication energy consumptions during the flocking process, it is impossible to apply this algorithm to engineering applications such as distributed sensing in mobile sensor networks. Considering that only partial agents can be informed of the virtual leader, Su *et al*. [18] reduced the communication energy consumption in Olfati-Saber's algorithm by adding a control indicator h_i.

The associate editor coordinating the review of this manuscript and approving it for publication was Jianxiang Xi.

Recently, the following studies closely related to this paper have been published. Zhan and Li [19] presented a centralized flocking algorithm via the model predictive control based on global position-only measurements for the first time, and further developed this algorithm to a distributed mechanism. Since the laser range finder cannot identify obstacles and robots, Sakai *et al.* [20] designed a flocking algorithm in which all the detected targets are viewed as obstacles. Although numerical simulations and experimental results were provided to verify the effectiveness of this algorithm, some limitations remain. For instance, the calculation difficulties for a single robot greatly increases during the flocking process. This work will get over the limitation later. In 2015, Semnani and Basir [21], benefiting from the advantages of both the flocking [17] and anti-flocking algorithms [22], proposed a semi-flocking algorithm to achieve multi-target tracking in large-scale surveillance systems. After that, Yuan *et al.* [23] developed a fully distributed semi-flocking algorithm that only requires local information on states of the agents (or sensors). To promote sustainable prosumer management in smart grids, from the perspective of complex network, Cao *et al.* [24] proposed a partially visible multi-agent system to achieve collective behavior of the prosumers. Obviously, the prosumers also follow Reynolds' rules during the flocking process. However, most of the above researches assume that the agents have the same social distancing (or equilibrium distance) and sensing radius. In fact, as a society, social distancing will vary depending on different cultural backgrounds, environments, industries, and personalities, etc. From the perspective of psychology, social distancing can be divided into the following three categories: public distancing, personal distancing, and intimate distancing [25]. Indeed, the social distancing of any particular person will vary in special cases. For example, during the fight against COVID-19, social distancing for everyone has increased by more than 2-fold compared with that observed during the normal periods [26]. Therefore, it is of great theoretical and practical significance for the research on the flocking of multi-agents with different social distancing and sensing radii. Note that the social distancing is proportional to the sensing radius (refer to [17]). For brevity, we will mention only the different social distancing later.

In this paper, considering the difference in social distancing among individuals, based on the extent of social distancing, a group composed of N mobile agents can be divided into multiple different subgroups. Especially, one of things we are very interested in is the collision avoidance between different subgroups during the flocking process. To explore the internal mechanism of this interesting problem, a novel flocking algorithm with multiple virtual leaders is proposed. The proposed algorithm is a modified version of the flocking algorithm provided by Olfaiti-Saber [17] and the semi-flocking algorithm proposed in [21]. Similarly, this algorithm does not explicitly distinguish between neighboring agents and obstacles. However, different from the work of Sakai *et al.* [20], from the perspective of differential game theory, the agents can either be cooperative or non-cooperative in our algorithm [27]–[29]. Thus, the flocking problem of different subgroups can be regarded as collision avoidance between neighboring agents, or obstacle avoidance between agents and virtual static/dynamic obstacles (the virtual obstacles will be illustrated in Sections II and V). In this way, to some extent, the calculation difficulties for a single agent (or robot) can be reduced. Furthermore, considering the complex environment that swarm robots or unmanned aerial vehicles (UAVs) may face when performing military missions such as surveillance, reconnaissance, and rescue, etc., we also investigate the flocking problem of multi-agents in both virtual static and dynamic obstacles environment.

The outline of this paper is organized as follows. Section II introduces some preliminary knowledge about graph theory. A novel flocking algorithm with multiple virtual leaders is designed in Section III. In Section IV, based on the Lyapunov stability theorem and LaSalle's invariance principle, the stability analysis of the proposed algorithm is proven. Numerical simulations are presented in Section V to illustrate the effectiveness of the proposed algorithm and the theoretical results. Finally, the conclusion is described in Section VI.

II. PRELIMINARIES AND PROBLEM FORMULATION

A. PRELIMINARIES OF GRAPH THEORY

Suppose that a group consists of N mobile agents. The interaction among these agents can be represented by a weighted undirected graph $G = (V, E, A)$, where $V = \{1, 2, \ldots, N\}$ is a vertex set, $E \subseteq \{(i, j) : i, j \in V, j \neq i\}$ is the edge set with vertexes of a junction, and the adjacency matrix $A = [a_{ij}]$ of the undirected graph G is defined as $a_{ij} = 1$, if $(i, j) \in E$, $a_{ij} = 0$ otherwise. Note that the adjacency matrix A is symmetric (i.e., $A^T = A$). The Laplacian matrix $L = [l_{ij}]$ is a $N \times N$ matrix, which is described by $L = D - A$, where the degree matrix $D \in \mathbb{R}^{N\times N}$ is a diagonal matrix with diagonal elements $d_{ii} = \sum_{j=1}^{N} a_{ij}$.

B. PROBLEM FORMULATION

Consider a group of N mobile agents moving in a two-dimensional Euclidean space with double-integrator dynamics, which is defined as follows:

$$\begin{cases} \dot{p}_i = v_i \\ \dot{v}_i = u_i \end{cases}, i = 1, 2, \ldots, N, \tag{1}$$

where $p_i, v_i \in \mathbb{R}^2$ are the position and velocity vector, respectively, of agent i, and $u_i \in \mathbb{R}^2$ is the control input (or control protocol). In this paper, we suppose that each agent is equal in size and mass, and has a limited sensing radius r (usually $r > 0$). Then, the neighboring set of agent i is described by

$$N_i = \{j \in V : \|p_j - p_i\| < r\}, \tag{2}$$

where $\|\cdot\|$ is the Euclidean norm in $\mathbb{R}^2$, and each agent can acquire the information of its neighboring agents, as shown

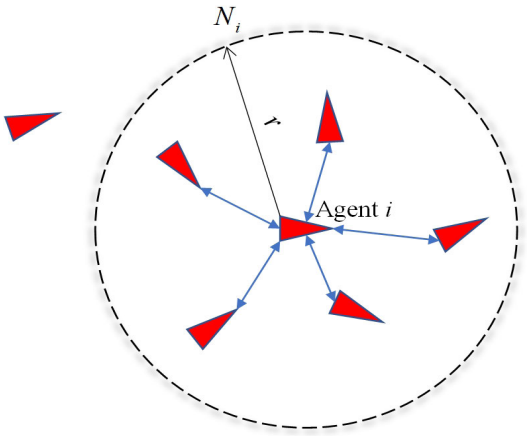

FIGURE 1. The schematic diagram of the neighboring set of agent i.

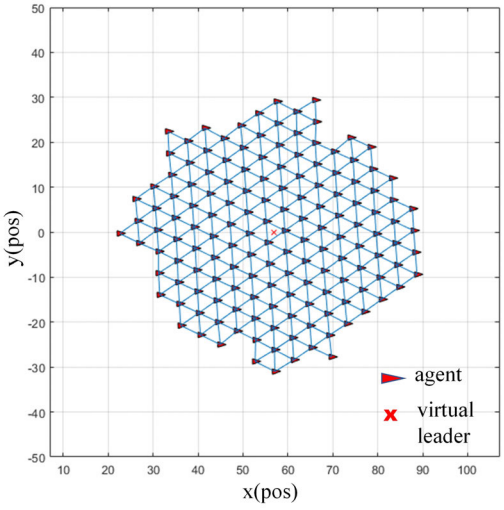

FIGURE 2. The illustration of an α-*lattice* flocking structure [17].

in Figure 1. According to the α-*lattice* flocking (see Figure 2) proposed in [17], the desired geometry of flocking requests that the distances between neighboring agents are equal. In other words, the distances should satisfy the following constraints:

$$\|p_j - p_i\| = d_e, \tag{3}$$

where $i = 1, 2, \ldots, N, \forall j \in N_i$. $d_e > 0$ represents the social distancing, and usually $d_e < r$.

Moreover, one $\gamma-agent$ can be viewed as the virtual leader (or group objective) of the multi-agent system, which drives all agents to move towards the same target and asymptotically match the same velocity. We assume that there are K ($1 \leq K \leq N$) virtual leaders, and each virtual leader abides by the following dynamics:

$$\begin{cases} \dot{p}_{\gamma k} = v_{\gamma k} \\ \dot{v}_{\gamma k} = f_{\gamma k}(p_{\gamma k}, v_{\gamma k}), \end{cases} \quad \gamma_k \in \{1, 2, \ldots, K\}, \tag{4}$$

where $p_{\gamma k}, v_{\gamma k}, f_{\gamma k} \in \mathbb{R}^2$ are the position, velocity, and control input, respectively, of the virtual leader γ_k. $(p_{\gamma k}(0), v_{\gamma k}(0)) = (p_d, v_d)$ denotes the initial state vector pairs. In Section V, we suppose that the virtual leader always moves at a constant velocity p_d along a fixed direction. Thus, the dynamic equation (4) is simplified as $p_{\gamma k}(0) = p_d$, $\dot{p}_{\gamma k} = v_d$. Besides, the main symbols of this paper are listed in Table 1.

TABLE 1. The main symbols of this paper.

Symbols	Descriptions
N	The number of agents
A	The $N \times N$ adjacency matrix
L	The $N \times N$ Laplacian matrix
$\mathbb{R}^2$	Two-dimensional real column space
N_i	The neighboring set of agent i
r	The sensing radius
d_e	The social distancing
K	The number of virtual leaders
f_α	The pair-wise action function
F_α	The pair-wise potential function
$N_{\gamma k}$	The number of agents tracking the virtual leader γ_k
$\tilde{V}_i$	The collective potential function

It is worth noting that this section does not explicitly distinguish between neighboring agents and obstacles. In [20], it was assumed that, for a robot, all the detected targets (including other robots) are viewed as obstacles. However, as a society, the interconnections between individuals are very complex, and impermanent. To obtain the maximum benefit, people may choose to cooperate or confront. With this in mind, in this paper, the agents can either be cooperative or non-cooperative. For example, from the perspective of differential game theory, when the agents i and j (i.e., $j = 1, \ldots, N, j \neq i$) have the same target, they choose to cooperate, and then, the agent j is viewed as the neighbors of agent i. But when the targets of the agents i and j are different, they are non-cooperative. At the moment, for the agent i, the agent j is viewed as a virtual dynamic/static obstacle. Therefore, the flocking problem of different subgroups can be regarded as collision avoidance between neighboring agents, or obstacle avoidance between the agents and the virtual static/dynamic obstacles. This complex phenomenon is the main research interest in this work. Accordingly, in the next section, a novel flocking algorithm with multiple virtual leaders is proposed to explore the internal mechanism of collision avoidance between different subgroups of multi-agents.

III. FLOCKING CONTROL ALGORITHM WITH MULTIPLE VIRTUAL LEADERS

As mentioned above, a novel flocking algorithm with multiple virtual leaders is considered in this section. The proposed algorithm is a modified version of the typical flocking algorithm [17] and the semi-flocking algorithm [21]. In 2006,

Olfati-Saber, inspired by Reynolds' rules, designed a typical flocking algorithm that has been extensively applied in fields such as mobile sensor networks and unmanned aircraft systems (UAS), etc. In [17], the control input u_i for agent i is made up of three components

$$u_i = u_i^g + u_i^d + u_i^\gamma, \tag{5}$$

where u_i^g, u_i^d are the gradient-based term and velocity consensus term, respectively, of the control input u_i. u_i^γ is navigational feedback to enable each agent to successfully track its virtual leader, which is defined as.

$$u_i^\gamma = \sum_{k=1}^{K} \frac{c_1(p_{\gamma k} - p_i) + c_2(v_{\gamma k} - v_i)}{N_{\gamma k}} \tag{6}$$

where $N_{\gamma k}$ represents the number of the agents tracking the virtual leader γ_k, and $c_1, c_2 > 0$.

Note that we are more focused on collision avoidance between different subgroups of multi-agents, rather than multi-target tracking of multi-agent systems. The semi-flocking algorithm proposed in [21] is mainly divided into the following two parts: the target searching mode and the target tracking mode. Whereas, for convenience, we neglect the target searching mode in this paper. In other words, we assume that different groups can be informed of their own virtual leaders. For example, in Section V, based on the extent of social distancing, a group $\mathbf{S}$, composed of N mobile agents, can be divided into the subgroups S_1 and S_2. We assume that the number of the subgroup S_1 are M $(1 < M < N)$, but the agents $i = M+1, \ldots, N$ for the subgroup S_2. γ_1 and γ_2 are the virtual leaders of the subgroups S_1 and S_2, respectively. Therefore, the navigational feedback u_i^γ is simplified as $u_i^\gamma = c_1(p_{\gamma 1} - p_i) + c_2(v_{\gamma 1} - v_i)$ for $i = 1, 2, \ldots, M$, but $u_i^\gamma = c_1(p_{\gamma 2} - p_i) + c_2(v_{\gamma 2} - v_i)$ for $i = M+1, M+2, \ldots, N$.

Moreover, to the best of our knowledge, a major limitation of the artificial potential function proposed in [16]-[18] is the local minima that deviate from the globally optimal goal, which may lead to unexpected failure during the flocking process. To overcome this limitation, based on the Lennard-Jones potential function [30] and the self-organization process [31], a simpler pair-wise action function is designed to simplify the interaction protocols between neighboring agents. More specifically, the control input (5) is modified as

$$u_i = \sum_{j \in N_i} f_\alpha(||p_j - p_i||)e_{ij} + \sum_{j \in N_i} a_{ij}(v_j - v_i) + \sum_{k=1}^{K} \frac{c_1(p_{\gamma k} - p_i) + c_2(v_{\gamma k} - v_i)}{N_{\gamma k}}, \quad i \in V, \tag{7}$$

where $e_{ij} = \frac{p_j - p_i}{\sqrt{1+\varepsilon||p_j - p_i||^2}}$, $\varepsilon \in (0, 1)$ is a value along the line connecting p_i to p_j, and a_{ij} is the element of the adjacency matrix A in Section II. The pair-wise action function $f_\alpha(x)$ is described by

$$f_\alpha(x) = \begin{cases} k_1\left(\frac{1}{x} - \frac{1}{d_e}\right), & x \le d_e \\ 0, x > r & \\ k_2(d_e - x)e^{\frac{(x-d_e)^2}{r}}, & d_e < x \le r, \end{cases} \tag{8}$$

where k_1 is the coefficient of repulsion and k_2 is the coefficient of attraction. The pair-wise action function $f_\alpha(x)$ can be shown in Figure 3 when the social distancing d_e is 5. The plot shows that the action force between neighboring agents is a repulsion for a short range, but an attraction for a long range. In particular, the pair-wise potential function $F_\alpha(x)$ is defined as $F_\alpha(x) = \int_{d_e}^{x} f_\alpha(s)ds$.

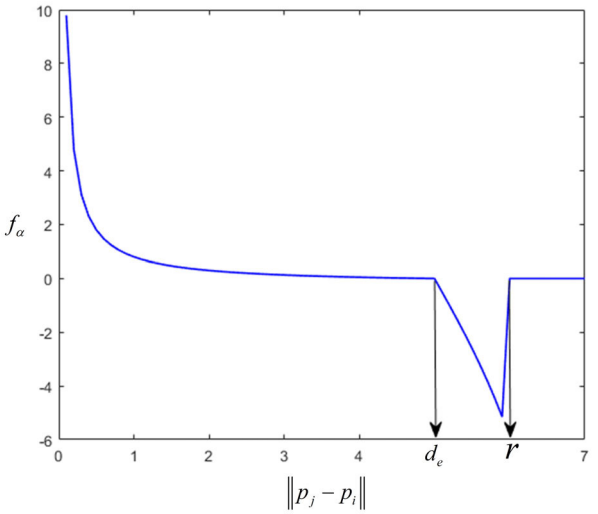

FIGURE 3. The pair-wise action function with a finite cut-off.

IV. STABILITY ANALYSIS

To analyze the collision avoidance capability and stability of the novel flocking algorithm with multiple virtual leaders, in this section, we first introduce a theorem related to the proposed algorithm. And then, prove this theorem by the Lyapunov stability theorem and LaSalle's invariance principle.

Theorem 1: Consider a group of N mobile agents with double-integrator dynamics (1), and each agent is affected by the control input (7). Suppose that the initial positions and velocities of all agents are chosen at random with the Gaussian distribution. Then, the following statement holds:

1) Flocking of the agents with the same virtual leader is formed asymptotically.
2) The velocity of the agents with the same virtual leader asymptotically become consistent.
3) No collisions occur between any neighboring agents.

Proof: We first define $\tilde{p}_i = p_i - p_{\gamma k}$, $\tilde{v}_i = v_i - v_{\gamma k}$ as the position error vector and velocity error vector, respectively.

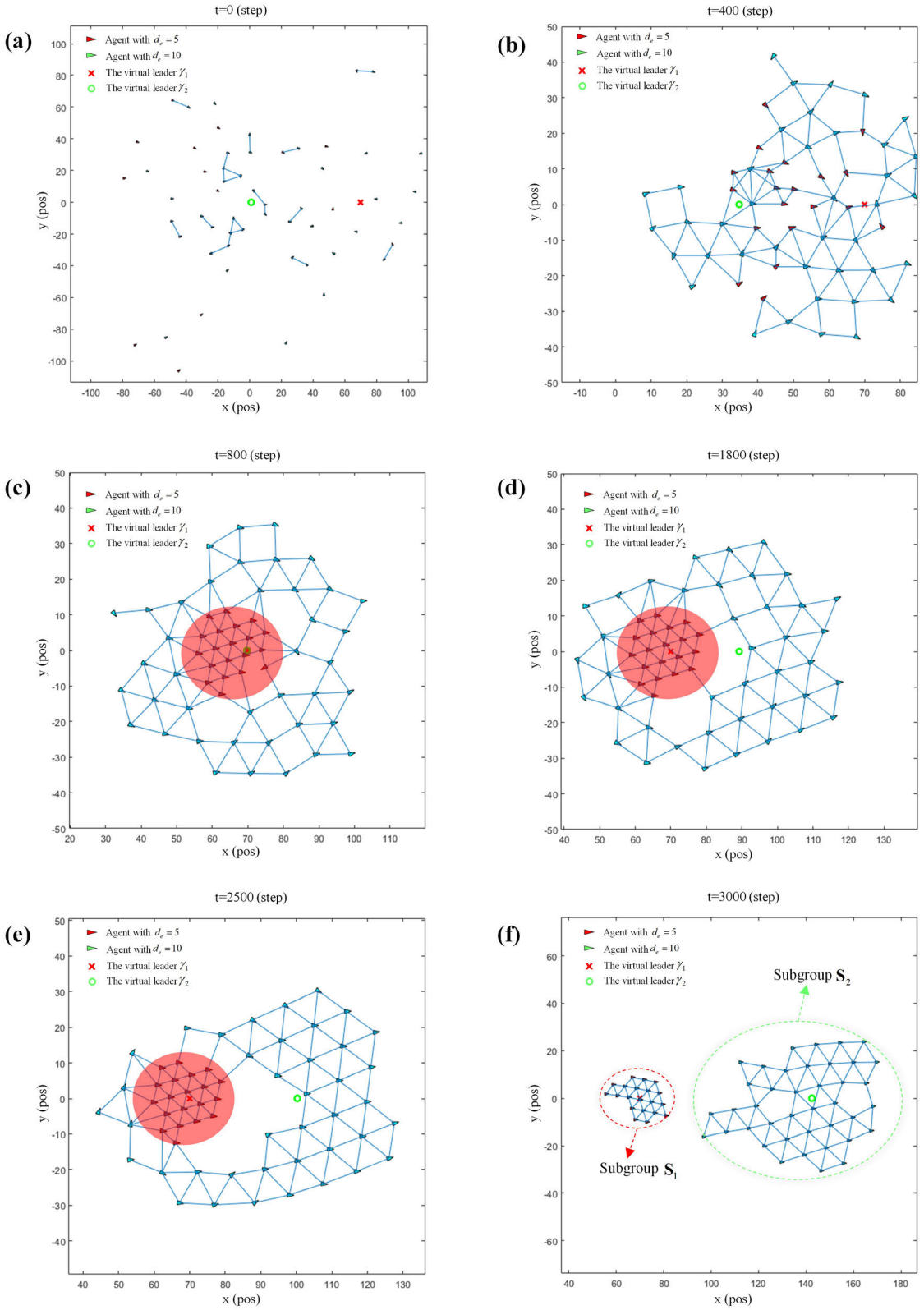

FIGURE 4. Flocking for two subgroups of multi-agents with different social distancing applying the control input (7) in 2-D. The red triangles belong to the subgroup S_1, whose social distancing is 5, whereas the green triangles represent the subgroup S_2, and its social distancing is 10. The number of subgroups S_1 and S_2 are 20 and 40, respectively. The red "lw" and green "O" denote the virtual leader, respectively, of the subgroup S_1 and S_2. An undirected edge connecting two agents means that they are neighbors of each other. (a) $t = 0$ step. (b) $t = 400$ step. (c) $t = 800$ sec. (d) $t = 1800$ step. (e) $t = 2500$ step. (f) $t = 3000$ step.

Accordingly, the error dynamics of agent i is given by

$$\begin{cases} \dot{\tilde{p}}_i = \tilde{v}_i \\ \dot{\tilde{v}}_i = u_i - u_{\gamma k}, \end{cases} \quad i = 1, 2, \ldots, N_{\gamma k}. \tag{9}$$

And then, let $p_{ij} = p_i - p_j$ and $\tilde{p}_{ij} = \tilde{p}_i - \tilde{p}_j$, clearly, $\tilde{p}_{ij} = p_{ij}$. Thus, the collective potential function V_i in [17] can be rewritten as

$$\begin{aligned} \tilde{V}_i(\tilde{p}_{ij}) &= \sum_{j \in V \setminus \{i\}} F_\alpha(||\tilde{p}_{ij}||) \\ &= \sum_{j \notin N_i, j \neq i} F_\alpha(r) + \sum_{j \in N_i} F_\alpha(||\tilde{p}_{ij}||). \end{aligned} \tag{10}$$

In the same way, the control input (7) of agent i is modified as

$$\begin{aligned} u_i = &\sum_{j \in N_i} f_\alpha(||\tilde{p}_{ij}||) e_{ij} + \sum_{j \in N_i} a_{ij}(\tilde{v}_j - \tilde{v}_i) \\ &- \frac{1}{N_{\gamma k}}(c_1 \tilde{p}_i + c_2 \tilde{v}_i), c_1, c_2 > 0. \end{aligned} \tag{11}$$

We choose an energy-like Lyapunov function as follows:

$$Q_k(\tilde{p}, \tilde{v}) = \frac{1}{2} \sum_{i=1}^{N_{\gamma k}} (U_i(\tilde{p}) + \tilde{v}_i^T \tilde{v}_i), \tag{12}$$

where

$$\begin{aligned} U_i(\tilde{p}) &= \sum_{j=1, j \neq i}^{N_{\gamma k}} F_\alpha(||\tilde{p}_{ij}||) + \frac{c_1}{N_{\gamma k}} \tilde{v}_i^T \tilde{v}_i \\ &= \tilde{V}_i(\tilde{p}_{ij}) + \frac{c_1}{N_{\gamma k}} \tilde{v}_i^T \tilde{v}_i, \end{aligned} \tag{13}$$

and $\tilde{p} = [\tilde{p}_1, \tilde{p}_2, \ldots, \tilde{p}_{N_{\gamma k}}]^T$, $\tilde{v} = [\tilde{v}_1, \tilde{v}_2, \ldots, \tilde{v}_{N_{\gamma k}}]^T$.

Thanks to the symmetry of the pair-wise potential function $F_\alpha(x)$ and the adjacency matrix A, it follows that

$$\frac{\partial F_\alpha}{\partial \tilde{p}_{ij}} = \frac{\partial F_\alpha}{\partial \tilde{p}_i} = -\frac{\partial F_\alpha}{\partial \tilde{p}_j}, \tag{14}$$

then

$$\frac{1}{2} \sum_{i=1}^{N_{\gamma k}} \dot{U}_i(\tilde{p}) = \sum_{i=1}^{N_{\gamma k}} (\tilde{v}_i^T \nabla_{\tilde{v}_i} \tilde{V}_i(\tilde{p}_{ij}) + \frac{c_1}{N_{\gamma k}} \tilde{v}_i^T \tilde{p}_i). \tag{15}$$

Consequently,

$$\begin{aligned} \dot{Q}_k(\tilde{p}, \tilde{v}) &= \frac{1}{2} \sum_{i=1}^{N_{\gamma k}} \dot{U}_i(\tilde{p}) + \sum_{i=1}^{N_{\gamma k}} \tilde{v}_i^T \dot{\tilde{v}}_i \\ &= -\tilde{v}^T [(L + \frac{c_2}{N_{\gamma k}} I_{N_{\gamma k}}) \otimes I_2] \tilde{v} \leq 0, \end{aligned} \tag{16}$$

where $\otimes$ is the Kronecker product notation, L denotes the Laplacian matrix in Section II, and $I_{N_{\gamma k}}, I_2$ are the identity matrices with corresponding dimensions.

Because L and $I_{N_{\gamma k}}$ are both positive semi-definite matrices, $L + \frac{c_2}{N_{\gamma k}} I_{N_{\gamma k}}$ is a positive semi-definite matrix as well. Hence, $\dot{Q}_k(\tilde{p}, \tilde{v}) \leq 0$, which means that $Q_k(\tilde{p}, \tilde{v}) = Q_k(t)$ is a non-increasing function over time t, and then $Q_k(t) \leq Q_{k0}$ for all $t \geq 0$. Note that Q_{k0} is the initial value of $Q_k(t)$. From Equations (12) and (13), we conclude that $c_1 \tilde{p}_i^T \tilde{p}_i \leq 2Q_{k0}$ for any agent i, which guarantees different α-*lattice* flocking of multiple subgroups with corresponding virtual leaders. Therefore, the part (i) is proven.

TABLE 2. Parameters of the proposed algorithm.

Parameters	Notation and Value
The social distancing	$d_e = 5$, 10, 15
The sensing radiuses	$r = 1.2 d_e$
Repulsion coefficient of the function (8)	$k_1 = 1$
Attraction coefficient of the function (8)	$k_2 = 5$
Coefficients of the control input (7)	$c_1 = c_2 = 1$
Simulation steps	t=3000~4500

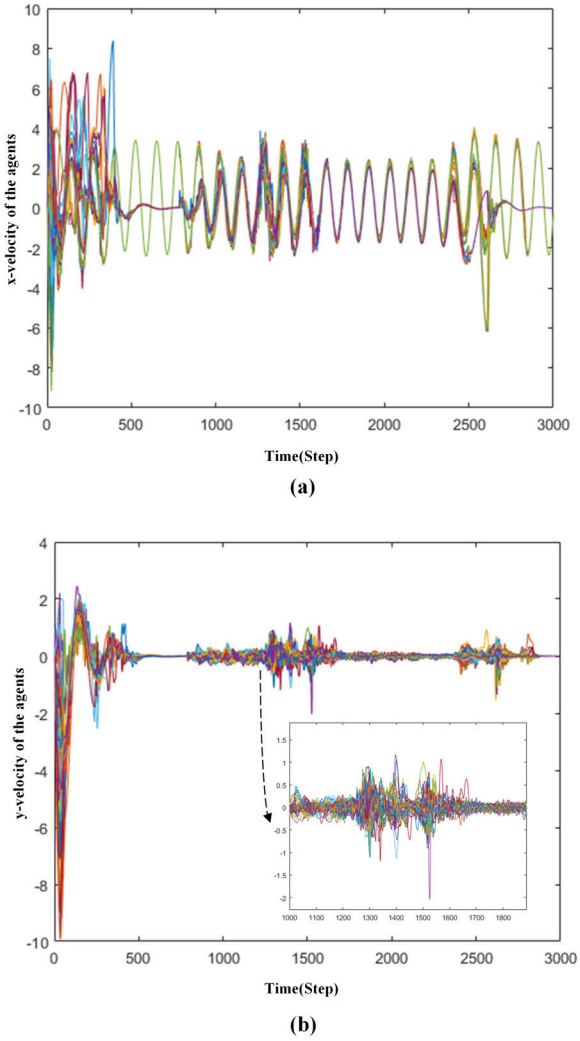

FIGURE 5. The velocities of all agents during the flocking process. (a) x-axis direction. (b) y-axis direction.

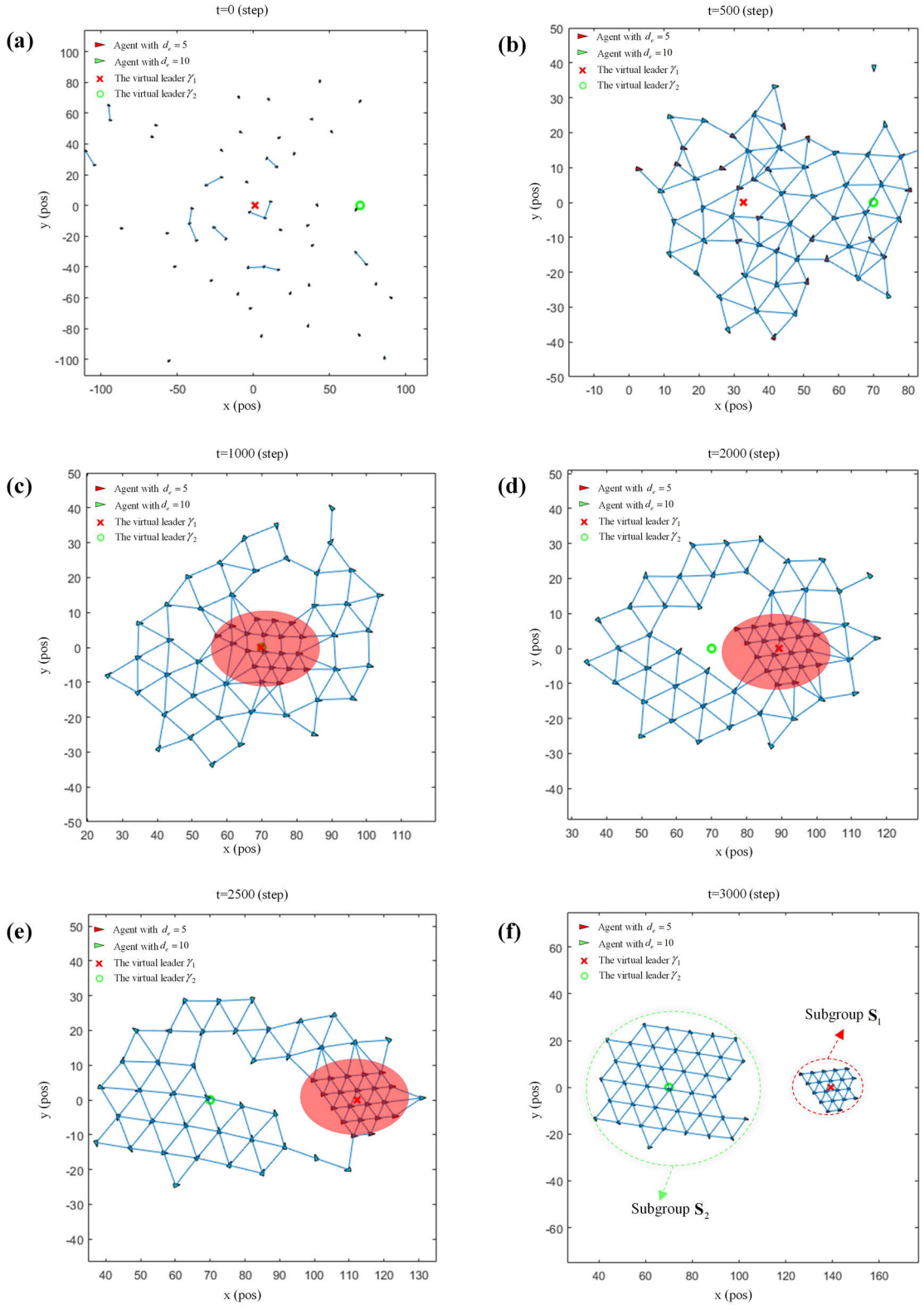

FIGURE 6. Flocking for two subgroups of multi-agents with different social distancing applying the control input (7) in 2-D. Compared with the simulation shown in Figure 4, this simulation exchanges the initial positions and dynamic equations of the virtual leader γ_1 and γ_2. Other parameters remain unchanged. (a) $t = 0$ step. (b) $t = 500$ step. (c) $t = 1000$ sec. (d) $t = 2000$ step. (e) $t = 2500$ step. (f) $t = 3000$ step.

Since $Q_k(t) > 0$ and $\dot{Q}_k(t) \leq 0$, we suppose that $\Omega = \{(\tilde{p}^T, \tilde{v}^T)^T | Q_k(t) \leq Q_0\}$ is an invariant set. According to LaSalle's invariance principle, the trajectories of all agents starting from Ω will converge to the largest set $\Psi = \{(\tilde{p}^T, \tilde{v}^T)^T | \dot{Q}_k(t) = 0\}$. From Equation (16), we have $\dot{Q}_k(\tilde{p}, \tilde{v}) = -\tilde{v}^T(L \otimes I_2)\tilde{v} - \frac{c_2}{N_{\gamma k}}\tilde{v}^T\tilde{v}$. As mentioned above, it is clear that $L \otimes I_2$ is also positive semi-definite. Therefore, we conclude that $\dot{Q}_k(\tilde{p}, \tilde{v}) = 0$ if and only if $\tilde{v}^T(L \otimes I_2)\tilde{v} = 0$ and $\tilde{v}^T\tilde{v} = 0$, which is equivalent to $v_1 \equiv \cdots \equiv v_{N_{\gamma k}} \equiv v_{\gamma k}$. Thus, the part (ii) is proven.

At last, we prove the part (iii) by contradiction. Assume that there are at least two agents colliding during the flocking process, we then acquire

$$\begin{aligned} Q(\tilde{p}, \tilde{v}) &= \sum_{k=1}^{K} Q_k(\tilde{p}, \tilde{v}) \\ &= \frac{1}{2}\sum_{k=1}^{K}\sum_{i=1}^{N_{\gamma k}}\left(\tilde{V}_i(\tilde{p}_{ij}) + \frac{c_1}{N_{\gamma k}}\tilde{v}_i^T\tilde{v}_i\right) + \frac{1}{2}\sum_{i=1}^{N}\tilde{v}_i^T\tilde{v}_i \\ &\geq \frac{1}{2}\sum_{k=1}^{K}\sum_{i=1}^{N_{\gamma k}}\tilde{V}_i(\tilde{p}_{ij}) \geq Q_0, \end{aligned} \tag{17}$$

which contradicts the condition $Q(t) \leq Q_0 = \sum_{k=1}^{K} Q_{k0}$. Hence, this hypothesis is not valid, and then, the part (iii) is proven.

V. SIMULATION RESULTS

In this section, numerical simulations are presented to validate the effectiveness of the proposed algorithm. All simulations are performed on a platform with the following configurations: 2.20 GHz CPU, 8.00 GB RAM, Windows 10, and MATLAB R2016b.

As mentioned in Section I, in real society, social distancing will vary depending on different cultural backgrounds, environments, industries, and personalities, etc. Considering the difference in social distancing among individuals, in this section, based on the extent of social distancing, a group **S**, composed of $N = 60$ mobile agents, can be divided into the subgroups S_1 and S_2. The initial positions of all the agents are chosen at random with the Gaussian distribution, whereas the initial velocities are zero. The number of the subgroup S_1 is 20, whose social distancing is 5, whereas the number of the subgroup S_2 is 40, and its social distancing is 10. The initial position and initial velocity of the virtual leader γ_1 are set as $p_{\gamma_1}(0) = [70, 0]^T$, and $v_{\gamma_1}(0) = [0, 0]^T$, respectively, and marked with a red "×". The initial position and initial velocity of the virtual leader γ_2 are set as $p_{\gamma_2}(0) = [0, 0]^T$, and $v_{\gamma_2}(0) = [0.5, 0]^T$, respectively, and marked with a green "O". Other parameters of the proposed algorithm are given in Table 2, which remain unchanged throughout this paper.

Figure 4 displays consecutive snapshots of the flocking for two subgroups of multi-agents with different social distancing applying the control input (7). From the perspective of differential game theory, when the virtual leader γ_2 asymptotically moves towards the virtual leader γ_1, the subgroups S_1 and S_2 have the same target. Each agent only needs to consider the social distancing with its neighboring agents during the flocking process. From Figure 4(a) to Figure 4(c), there are increasing numbers of agents connected together, but at a certain distance (i.e., the social distancing). Then, the subgroups S_1 and S_2 form an irregular flocking (note that this is different from the traditional α-*lattice* flocking, in the next, we will explain the reason), as shown in Figure 4(c). Obviously, no collisions occurred. However, when the virtual leader γ_2 overtakes the virtual leader γ_1, since the subgroup S_1 successfully tracks the virtual leader γ_1, it no longer moves. At this time, for the subgroup S_2, the subgroup S_1 is viewed as a virtual static obstacle represented by a translucent red ellipse (includes the following translucent green ellipse). From Figure 4(d) to Figure 4(f), it is shown that there are no collisions with the virtual static obstacle or other neighboring agents, and finally, forms two different α-*lattice* flocking.

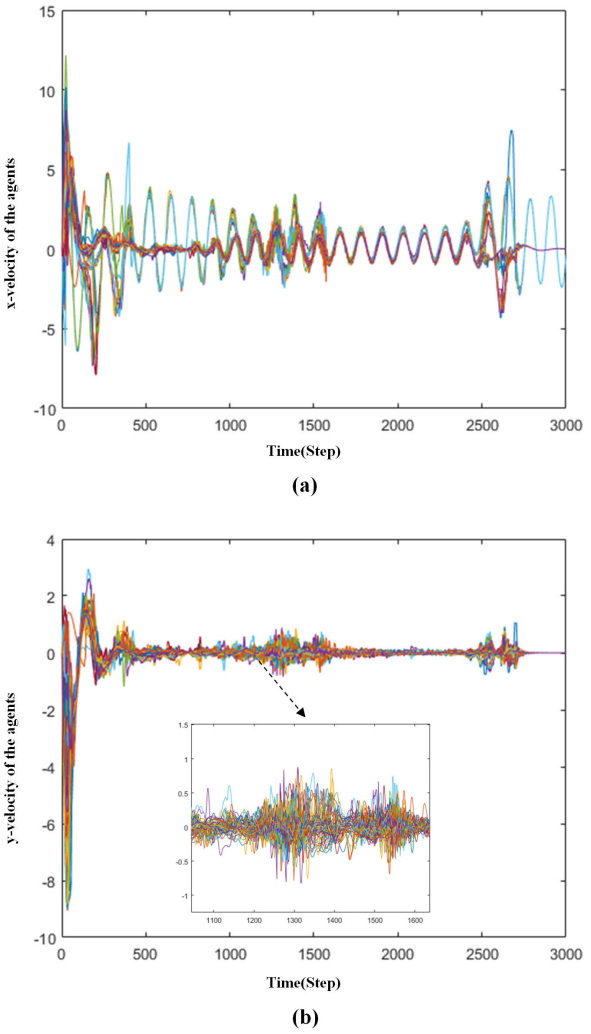

FIGURE 7. The velocities of all agents during the flocking process (simulation in Figure 6). (a) x-axis direction. (b) y-axis direction.

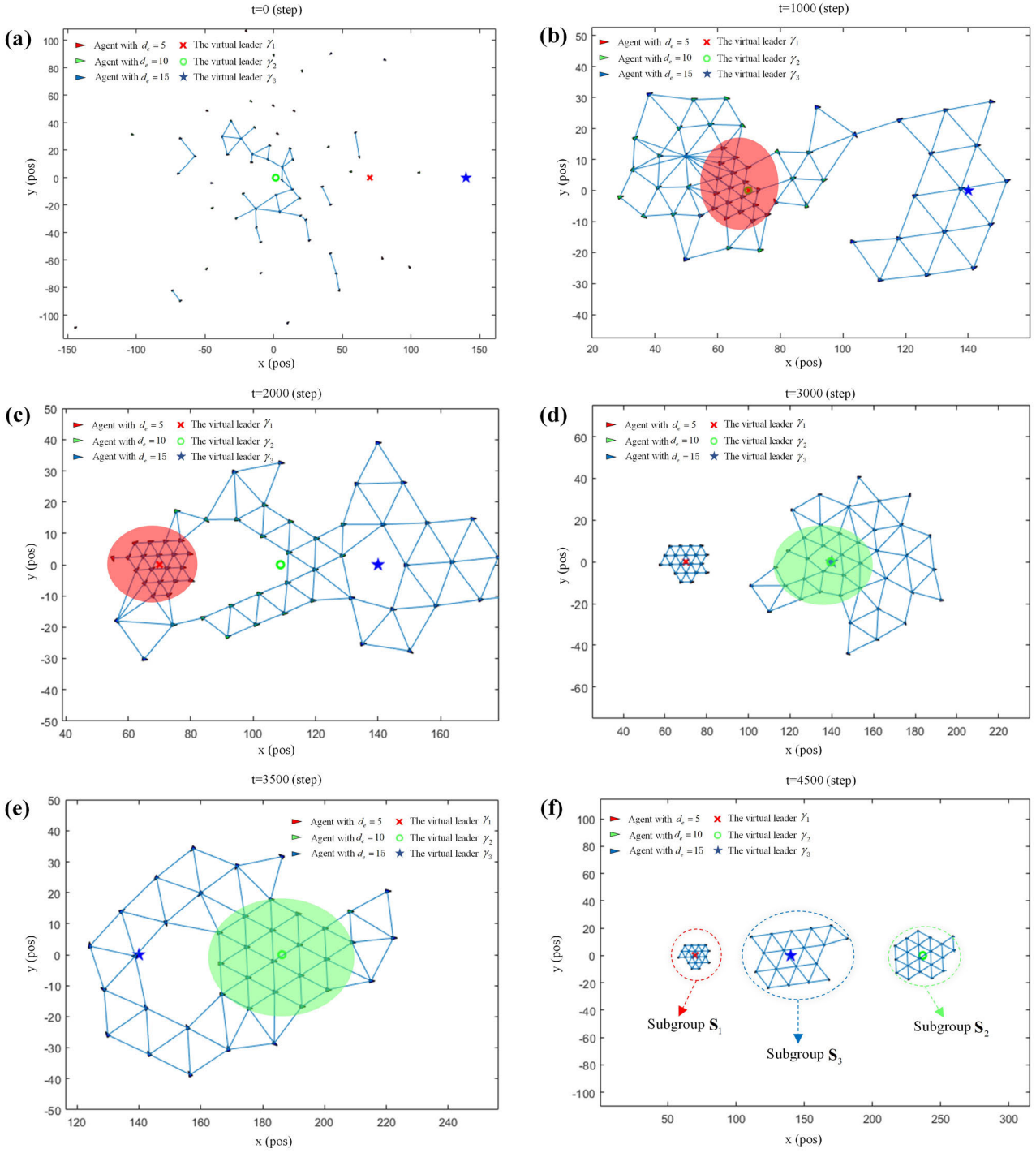

FIGURE 8. Flocking for three subgroups of multi-agents with different social distancing applying the control input (7) in 2-D. The red triangles belong to the subgroup S_1, whose social distancing is 5. The green triangles represent the subgroup S_2, whose social distancing is 10. Whereas the blue triangles denote the subgroup S_3, and its social distancing is 15. The number of three subgroups is equal to 20, respectively. The red "lw" and green "o" denote the virtual leader, respectively, of the subgroup S_1 and S_2, whereas the blue star represents the virtual leader of the subgroup S_3. An undirected edge connecting two agents means that they are neighbors of each other. (a) $t = 0$ step. (b) $t = 1000$ step. (c) $t = 2000$ sec. (d) $t = 3000$ step. (e) $t = 3500$ step. (f) $t = 4500$ step.

The velocities of multi-agents during the above simulation are further shown in Figure 5. The graph shows that the velocities in the x-axis direction and y-axis direction gradually converge to a constant set, respectively, when the subgroups S_1 and S_2 have the same target. Then, after the subgroup S_2 is regarded as a virtual static obstacle, the velocities begin to oscillate

during the obstacle avoidance process, and finally, converge back to a constant set. Accordingly, the above phenomena are completely consistent with our predictions of *Theorem 1* in Section IV.

From another perspective, Figure 4 can be regarded as a flocking problem of multi-agents in a virtual static obstacle environment. However, in practice, the obstacles are not only static, but also may be dynamic. Therefore, we next exchange the initial positions and dynamic equations of the subgroups S_1 and S_2. In other words, the initial position and velocity of the virtual leader γ_1 are set as $p_{\gamma_1}(0) = [0, 0]^T$, and $v_{\gamma_1}(0) = [0.5, 0]^T$, respectively. The initial position and velocity of the virtual leader γ_2 are set as $p_{\gamma_2}(0) = [70, 0]^T$, and $v_{\gamma_2}(0) = [0, 0]^T$, respectively. The remaining parameters remain fixed. Figure 6 displays consecutive snapshots of the flocking of multi-agents in a virtual dynamic obstacle environment. From Figure 6(a) to Figure 6(c), we can find that its trajectory is similar to Figure 4, when the subgroups S_1 and S_2 have the same target. However, when the virtual leader γ_1 overtakes the virtual leader γ_2, for the subgroup S_2, the subgroup S_1 can be viewed as a virtual dynamic obstacle at the moment. From Figure 6(d) to Figure 6(f), it is clear that there are no collisions with the virtual dynamic obstacle or other neighboring agents. Similarly, Figure 7 reveals that the velocity consensus is achieved during the flocking process.

The above simulations demonstrate the effectiveness of the proposed algorithm in the flocking for two subgroups of multi-agents with collision avoidance capability. Note that the above simulations only apply to the case where the obstacle is dynamic or static, respectively. However, when swarm robots or unmanned aerial vehicles (UAVs) perform military missions such as surveillance, reconnaissance or rescue, and so on, the environment they face may be more complex. In other words, there are both static and dynamic obstacles. Therefore, we then divide the group $\mathbf{S}$ into the following three subgroups S_1, S_2 and S_3 to help simulate the flocking of multi-agents in this complex environment.

Figure 8 displays consecutive snapshots of the flocking of multi-agents in both virtual static and dynamic obstacles environment. The number of each subgroup is equal to 20. The social distancing of the subgroup S_3 is 15. The initial position and velocity of the virtual leader γ_3 are set as $p_{\gamma_3}(0) = [140, 0]^T$, and $v_{\gamma_3}(0) = [0, 0]^T$, respectively, and marked with a blue star. The initial position and velocity of the virtual leader γ_1 are set as $p_{\gamma_1}(0) = [70, 0]^T$, and $v_{\gamma_1}(0) = [0, 0]^T$, respectively. The initial position and velocity of the virtual leader γ_2 are set as $p_{\gamma_2}(0) = [0, 0]^T$, and $v_{\gamma_2}(0) = [0.5, 0]^T$, respectively. Other parameters remain unchanged (include the social distancing of the subgroups S_1 and S_2). From Figure 8(a) to Figure 8(c), for the subgroups S_2 and S_3, the subgroup S_1 can be regarded as a virtual static obstacle when the virtual leader γ_2 overtakes the virtual leader γ_1. Whereas from Figure 8(d) and Figure 8(e), for the subgroup S_3, the subgroup S_2 is viewed as a virtual dynamic obstacle when the virtual leader γ_2 overtakes the virtual leader γ_3, and finally, forms three different α-*lattice* flocking,

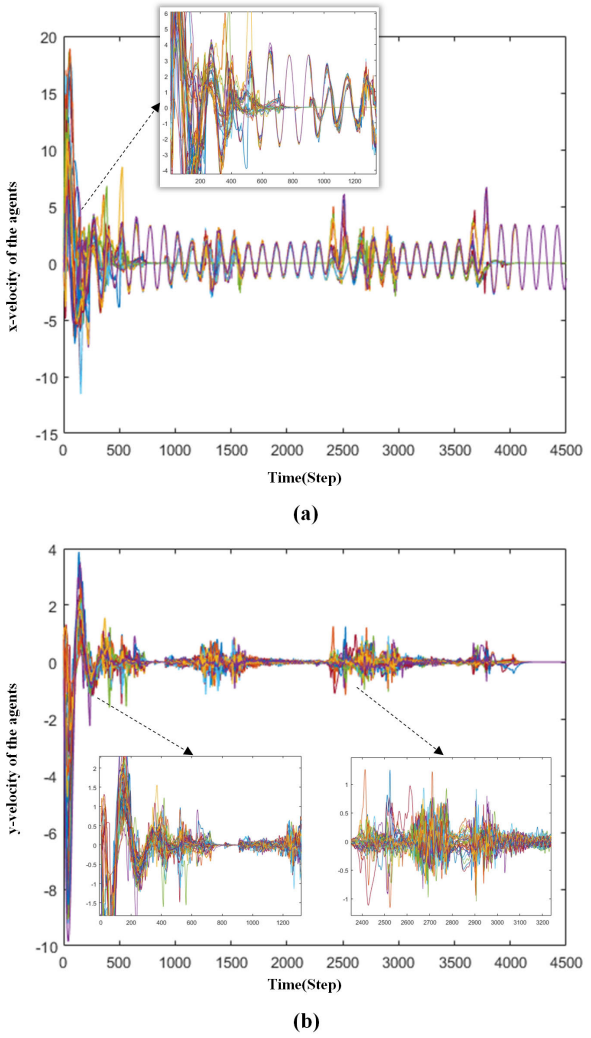

FIGURE 9. The velocities of all agents during the flocking process (simulation in Figure 8). (a) x-axis direction. (b) y-axis direction.

as shown in Figure 8(f). Apparently, the graph shows that no collisions occurred during the whole flocking process. Moreover, Figure 9 indicates that the velocity consensus is also achieved, where the oscillation curves correspond to the collision avoidance process between different subgroups.

From the above simulations, we can find that the subgroup with large social distancing (e.g., the subgroup S_3) always actively avoids the subgroup with small social distancing (e.g., the subgroup S_1 or S_2), and especially, this is not related to the dynamic equation of the corresponding virtual leaders. In addition, it is worth noting that the formed flocking structure (i.e., Figure 4(c) and Figure 6(c)) is different from the traditional α-*lattice* structure, when different subgroups have the same target. What causes these phenomena? The pair-wise action function f_α with different social distancing is shown in Figure 10. Suppose that the social distancing of agent i is d_e, whereas the agent j has a larger social distancing (i.e., $2d_e$ and $3d_e$). The graph shows that, if $\|p_j - p_i\| = d_e$,

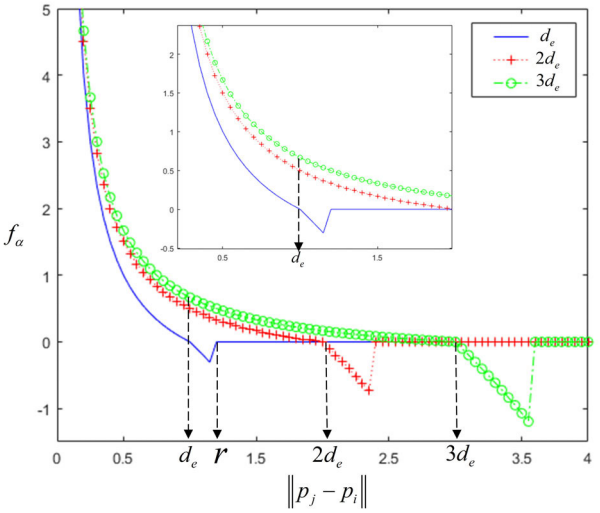

FIGURE 10. The action force function with different social distancing.

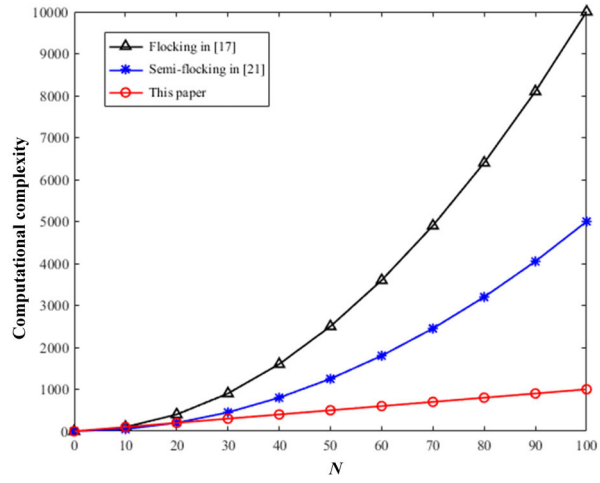

FIGURE 11. Comparison of computational complexity with different flocking algorithms.

the action force f_α^i of agent i is zero, and then, it stays at rest. However, for the agent j, its action force $f_\alpha^j > 0$, which is the repulsive force. Since the repulsive force, the agent j will gradually move away from the agent i until its action force is zero. Therefore, the irregular flocking is formed, as shown in Figure 4(c). Figure 10 reveals that social distancing d_e plays a key role in the flocking of multi-agents. In other words, the subgroup with small social distancing has a stronger cohesive force than the other with the large one.

Figure 11 shows the comparison of computational complexity with different flocking algorithms. As Figure 11 illustrates, the proposed algorithm demonstrates lower computational complexity than the other two algorithms, with respect to the number of agents. Therefore, we can conclude that the proposed algorithm is simple, yet effective for exploring the internal mechanism of collision avoidance between different subgroups of multi-agents.

VI. CONCLUSION

Most existing studies of flocking for multi-agent systems assumed that the agents have the same social distancing. However, as a society, social distancing will vary depending on different cultural backgrounds, environments, industries, and personalities, etc. Considering the difference in social distancing among individuals, in this paper, according to the extent of the social distancing, a group S, composed of N mobile agents, was divided into multiple different subgroups. Then, a novel flocking algorithm with multiple virtual leaders was proposed to research the flocking problem of multi-agents with different social distancing. The proposed algorithm is an improvement on the traditional flocking and semi-flocking algorithms. Especially, from the differential game theory, the flocking problem of different subgroups could be regarded as collision avoidance between neighboring agents, or obstacle avoidance between the agents and the virtual static/dynamic obstacles. Finally, numerical simulations demonstrated the effectiveness of the proposed algorithm and theoretical results. This work indicated that the social distancing plays a key role in the flocking of multi-agents, especially in multiple different subgroups of multi-agents.

As future works, we intend to consider the impact of individual heterogeneity on the flocking for multi-agent systems, rather than just being limited to different social distancing between individuals, and to explore how to apply the proposed algorithm to extremely large-scale datasets.

REFERENCES

[1] E. Shaw, "Fish in schools," *Natural His.*, vol. 84, no. 8, pp. 40–45, 1975.
[2] H. Ling, G. E. Mclvor, J. Westley, K. van der Vaart, R. T. Vaughan, A. Thornton, and N. T. Ouellette, "Behavioural plasticity and the transition to order in jackdaw flocks," *Nature Commun.*, vol. 10, no. 1, pp. 1–7, Nov. 2019.
[3] H. Ling, G. E. Mclvor, K. van der Vaart, R. T. Vaughan, A. Thornton, and N. T. Ouellette, "Costs and benefits of social relationships in the collective motion of bird flocks," *Nature Ecol. Evol.*, vol. 3, no. 6, pp. 943–948, May 2019.
[4] W. Yuan, N. Ganganath, C.-T. Cheng, G. Qing, F. C. M. Lau, and Y. Zhao, "Path-Planning-Enabled semiflocking control for multitarget monitoring in mobile sensor networks," *IEEE Trans. Ind. Informat.*, vol. 16, no. 7, pp. 4778–4787, Jul. 2020.
[5] S. Chen, H. Pei, Q. Lai, and H. Yan, "Multitarget tracking control for coupled heterogeneous inertial agents systems based on flocking behavior," *IEEE Trans. Syst., Man, Cybern. Syst.*, vol. 49, no. 12, pp. 2605–2611, Dec. 2019.
[6] X. Luo, S. Li, and X. Guan, "Flocking algorithm with multi-target tracking for multi-agent systems," *Pattern Recognit. Lett.*, vol. 31, no. 9, pp. 800–805, Jul. 2010.
[7] H. Zhao, H. Liu, Y.-W. Leung, and X. Chu, "Self-adaptive collective motion of swarm robots," *IEEE Trans. Autom. Sci. Eng.*, vol. 15, no. 4, pp. 1533–1545, Oct. 2018.
[8] Z. Miao, J. Yu, J. Ji, and J. Zhou, "Multi-objective region reaching control for a swarm of robots," *Automatica*, vol. 103, pp. 81–87, May 2019.
[9] Y. Zhou, H. Hu, Y. Liu, S.-W. Lin, and Z. Ding, "A distributed method to avoid higher-order deadlocks in multi-robot systems," *Automatica*, vol. 112, Feb. 2020, Art. no. 108706.

[10] G. Vásárhelyi, C. Virágh, G. Somorjai, T. Nepusz, A. E. Eiben, and T. Vicsek, "Optimized flocking of autonomous drones in confined environments," *Sci. Robot.*, vol. 3, no. 20, Jul. 2018, Art. no. eaat3536.
[11] F. Dai, M. Chen, X. Wei, and H. Wang, "Swarm intelligence-inspired autonomous flocking control in UAV networks," *IEEE Access*, vol. 7, pp. 61786–61796, 2019.
[12] W. Zhao, H. Chu, M. Zhang, T. Sun, and L. Guo, "Flocking control of fixed-wing UAVs with cooperative obstacle avoidance capability," *IEEE Access*, vol. 7, pp. 17798–17808, 2019.
[13] C. W. Reynolds, "Flocks, herds and schools: A distributed behavioral model," *ACM SIGGRAPH Comput. Graph.*, vol. 21, no. 4, pp. 25–34, Aug. 1987.
[14] T. Vicsek, A. Czirók, E. Ben-Jacob, I. Cohen, and O. Shochet, "Novel type of phase transition in a system of self-driven particles," *Phys. Rev. Lett.*, vol. 75, no. 6, pp. 1226–1229, Aug. 1995.
[15] A. Jadbabaie, J. Lin, and A. S. Morse, "Coordination of groups of mobile autonomous agents using nearest neighbor rules," *IEEE Trans. Autom. Control*, vol. 48, no. 6, pp. 988–1001, Jun. 2003.
[16] H. G. Tanner, "Flocking with obstacle avoidance in switching networks of interconnected vehicles," in *Proc. IEEE Int. Conf. Robot. Autom. (ICRA)*, New Orleans, LA, USA, Apr./May 2004, pp. 3006–3011.
[17] R. Olfati-Saber, "Flocking for multi-agent dynamic systems: Algorithms and theory," *IEEE Trans. Autom. Control*, vol. 51, no. 3, pp. 401–420, Mar. 2006.
[18] H. Su, X. Wang, and Z. Lin, "Flocking of multi-agents with a virtual leader," *IEEE Trans. Autom. Control*, vol. 54, no. 2, pp. 293–307, Feb. 2009.
[19] J. Zhan and X. Li, "Flocking of multi-agent systems via model predictive control based on position-only measurements," *IEEE Trans. Ind. Informat.*, vol. 9, no. 1, pp. 377–385, Feb. 2013.
[20] D. Sakai, H. Fukushima, and F. Matsuno, "Flocking for multirobots without distinguishing robots and obstacles," *IEEE Trans. Control Syst. Technol.*, vol. 25, no. 3, pp. 1019–1027, May 2017.
[21] S. H. Semnani and O. A. Basir, "Semi-flocking algorithm for motion control of mobile sensors in large-scale surveillance systems," *IEEE Trans. Cybern.*, vol. 45, no. 1, pp. 129–137, Jan. 2015.
[22] Y.-Q. Miao, A. Khamis, and M. S. Kamel, "Applying anti-flocking model in mobile surveillance systems," in *Proc. Int. Conf. Auto. Intell. Syst. (AIS)*, Jun. 2010, pp. 1–6.
[23] W. Yuan, N. Ganganath, C.-T. Cheng, G. Qing, and F. C. M. Lau, "Semi-Flocking-Controlled mobile sensor networks for dynamic area coverage and multiple target tracking," *IEEE Sensors J.*, vol. 18, no. 21, pp. 8883–8892, Nov. 2018.
[24] J. Cao, Z. Bu, Y. Wang, H. Yang, J. Jiang, and H.-J. Li, "Detecting prosumer-community groups in smart grids from the multiagent perspective," *IEEE Trans. Syst., Man, Cybern. Syst.*, vol. 49, no. 8, pp. 1652–1664, Aug. 2019.
[25] N. S. Rieger and J. P. Christianson, "Vigilance in a time of social distancing," *Neuropsychopharmacology*, vol. 0, pp. 1409–1410, Apr. 2020.
[26] R. West, S. Michie, G. J. Rubin, and R. Amlôt, "Applying principles of behaviour change to reduce SARS-CoV-2 transmission," *Nature Hum. Behaviour*, vol. 4, no. 5, pp. 451–459, May 2020.
[27] T. Mylvaganam, M. Sassano, and A. Astolfi, "A differential game approach to multi-agent collision avoidance," *IEEE Trans. Autom. Control*, vol. 62, no. 8, pp. 4229–4235, Aug. 2017.
[28] G. Piyush, B. Kaivalya, and E. A. Theodorou, "A mean-field game model for homogeneous flocking," *J. Math. Phys.*, vol. 28, pp. 061103–061111, May 2018.
[29] H. Yang, Z. Bu, Y. Wang, X. Xiong, and C. Zhang, "A non-cooperative game model for overlapping community detection in social networks," in *Proc. IEEE 20th Int. Conf. Inf. Reuse Integr. Data Sci. (IRI)*, Angeles, CA, USA, Jul. 2019, pp. 299–306.
[30] W. W. Wood and F. R. Parker, "Monte Carlo equation of state of molecules interacting with the Lennard-Jones potential. I. A supercritical isotherm at about twice the critical temperature," *J. Chem. Phys.*, vol. 27, no. 3, pp. 720–733, Aug. 2004.
[31] J.-M. Lehn, "Toward self-organization and complex matter," *Science*, vol. 295, no. 5564, pp. 2400–2403, Mar. 2002.

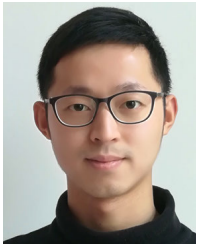

HUI WEI was born in Sichuan, China, in 1996. He received the B.S. degree from the Yingkou Institute of Technology, China, in 2018. He is currently pursuing the M.S. degree with the University of Science and Technology Liaoning, China. His current research interests include complex systems and coordinated control of multi-agent systems.

XUE-BO CHEN received the B.S. and M.S. degrees from the Anshan Institute of Iron and Steel Technology, China, in 1982 and 1985, respectively, and the Ph.D. degree from the University of Belgrade, Yugoslavia, in 1994, all in electrical engineering. From December 1997 to May 1998, he was a Research Associate with the School of Engineering, Santa Clara University, Santa Clara, CA, USA. He has been with the University of Science and Technology Liaoning, since 1982, where he is currently a Professor of control engineering. His current research interests include complex systems, group robot systems, and swarm intelligence.